



# Functional finishing of woven fabric with reduced graphene oxide nanosheets decorated with Ag-N doped titanium dioxide nanoparticles

Simran Sharma, Vinay Midha<sup>a</sup> & Sushma Verma

Department of Textile Technology, Dr B R Ambedkar National Institute of Technology, Jalandhar 144 011, India

Received 25 August 2020; revised received and accepted 15 May 2021

An innovative approach has been made to impart self-cleaning and antibacterial properties to woven fabrics. Reduced graphene oxide/Ag-N TiO<sub>2</sub> nanocomposites are successfully prepared by simple mixing and sonication for finishing of woven fabric with prepared nanocomposites. The physiochemical properties of prepared samples are analysed by X-ray diffraction, UV-Visible spectroscopy, Field emission scanning electron microscope and Fourier transform infrared radiation spectroscopy. The prepared nanocomposite (rGO/ 1% Ag-N TiO<sub>2</sub>) shows lower bandgap of 2.3 eV as compared to individual nanomaterials, and hence the improved photocatalytic performance, leading to high self-cleaning and antibacterial activity.

**Keywords:** Antibacterial activity, Cotton, Functional finishing, Polyester/cotton woven fabric, Reduced graphene oxide/Ag-N TiO<sub>2</sub> nanocomposite, Self-cleaning property

## 1 Introduction

Titanium dioxide nanoparticles have recently become an area of research in textiles for their photocatalytic activity and thus for imparting self-cleaning finish. Its non-toxicity and multifunctional properties make it suitable for application on textile products<sup>1</sup>. Ceramic was the first photocatalytic self-cleaning material discovered by Heller *et al*<sup>2</sup>. and Sunada *et al*.<sup>3</sup> in early 1990's. Photocatalytic antimicrobial property of titanium dioxide coated materials was discovered by scientists after three years, when titanium dioxide completely disintegrated *Escherichia coli* under UV radiations<sup>4</sup>. Progressive approach in nanotechnology has opened new doors for the development of new nanomaterials. Graphene is a one-atom-thick planar sheet of sp<sup>2</sup> bonded carbon atoms densely packed into 2D honeycomb crystal lattice<sup>5</sup>. Graphene oxide is considered to be the most important derivative of grapheme, as it is an atomic layer thick and has a wide range of functional groups, like epoxy, hydroxyl and carboxyl<sup>6,7</sup>. Recently, research studies have found increased photocatalytic performance with the incorporation of graphene derivatives in titanium dioxide.

TiO<sub>2</sub>/Graphene oxide nanocomposite prepared by simple mixing and sonication showed excellent photocatalytic and antibacterial properties<sup>8</sup>.

Furthermore, cotton fibres treated with graphene oxide decorated with Fe, N-doped TiO<sub>2</sub> particles for use in industrial self-cleaning and biocompatible textiles are have been prepared by researchers. TiO<sub>2</sub> co-doped with metals and non-metals is extensively being investigated for improving photocatalytic and antibacterial performance. On the other hand, attachment of TiO<sub>2</sub> nanoparticles on two-dimensional graphene oxide sheets is also being studied. Attachment of TiO<sub>2</sub> and graphene oxide can occur through the bonding of the free electrons existing on the TiO<sub>2</sub> surface with unpaired  $\pi$  electrons of the carbon atoms to form a Ti-O-C structure. These composites increase visible light wavelength absorption due to graphene's highly conjugated structure that forms Ti-O-C chemical bonds, thereby reducing TiO<sub>2</sub> band gap due to carbon doping<sup>9</sup>. On the same line of research, effects of reduced graphene oxide/Ag-N TiO<sub>2</sub> coating on 35/65 polyester/cotton woven fabric are studied. In this study, reduced graphene oxide/Ag-N TiO<sub>2</sub> nanocomposites are synthesized and coated on the surface of polyester/cotton woven fabric to observe the self-cleaning and antibacterial effects.

## 2 Materials and Methods

### 2.1 Synthesis and Characterization of Ag-N TiO<sub>2</sub>

Titanium (IV) isopropoxide (TTIP), ethanol, silver nitrate and urea are procured from Sigma Aldrich, and distilled water is used throughout the study. Ag-N

<sup>a</sup>Corresponding author.  
E-mail: midhav@rediffmail.com

doped TiO<sub>2</sub> is synthesized in the laboratory via low temperature sol gel route. Twenty-five millilitre (25 mL) TTIP is added dropwise to 75 mL ethanol with continuous stirring for 2 h to make the Solution A. Nitric acid is added to 375 mL of water for maintaining the pH of 2 along with required amount of silver nitrate to make Solution B. Solution A is then added dropwise to Solution B at 25±2 °C with constant stirring for 2.5h. Solution is then allowed to dry at a constant rate of stirring at 80°C until solution is converted into gel, which then forms nanoparticles. Synthesized particles are dried at 100°C and calcined at 550°C for 4h to produce Ag doped TiO<sub>2</sub><sup>10-13</sup>. To produce Ag-N TiO<sub>2</sub>, the required amount of urea is sonicated in water for 30 min and prepared Ag TiO<sub>2</sub> particles are added to the solution and sonicated for 1 hour. After uniform dispersion of particles in water, they are dried at 100°C and calcined at 400°C<sup>14</sup>. The structural characterization of nanoparticles is done by X-ray diffraction (Panalytical X-ray diffractometer), Fourier Transform Infrared spectroscopy (Aligent Technologies Cary 630 Spectrophotometer), UV-Visible spectroscopy (Analytik Jena UV-spectrophotometer) and FE-SEM (Hitachi SU8000 UHR cold emission FE-SEM microscope.). Reduced graphene oxide is obtained from Nanoinnova Technologies SL with particle size 5µm and 3-6nm thickness.

## 2.2 Treatment of Fabric with Nanocomposite

Bleached plain weave 35/65 polyester/cotton fabric with warp and weft yarn density of 50 yarns/inch and 44 yarns/inch respectively, and fabric weight of 170 g/m<sup>2</sup> is used. Reduced graphene oxide and Ag-N TiO<sub>2</sub> nanocomposites are prepared by simple mixing and sonication. Different amounts of Ag-N doped TiO<sub>2</sub> and reduced graphene oxide, according to the Box Behnken design are sonicated for 1h at 50°C, as shown in Table 1. Fabric samples are immersed in prepared suspension for 1h at 80°C and then kept in the oven for 15 min at 100°C for fixation of nanocomposite onto the fabric<sup>8</sup>.

## 2.3 Characterization of Photocatalyst- treated Fabrics

Surface characteristics of nanocomposite coated samples are studied using Hitachi SU8000 UHR Cold-Emission FE-SEM Microscope, and evaluation of photocatalytic performance is done by measuring color strength of fabrics before and after staining on Datacolor Check LAV portable color control system in the form of color value as studied by Absorption

Table 1 — Experimental runs according to Box-Behnken design

% doping (X <sub>1</sub> )	Amount of Ag-N TiO <sub>2</sub> ,% (owf) (X <sub>2</sub> )	Amount of rGO, % (owf) (X <sub>3</sub> )	% Decrease in K/S value	
			Coffee stain	Methylene Blue
1	1	0.3	92.71	82.11
2	1	0	78.94	73.16
2	0.55	0.3	83.46	74.71
3	0.55	0.0	68.83	63.12
2	0.1	0.6	64.71	54.7
3	1	0.3	90.16	81.42
2	1	0.6	82.9	74.53
1	0.55	0.6	77.96	72.46
2	0.55	0.3	81.65	75.42
2	0.55	0.3	82.19	74.11
3	0.55	0.6	75.68	69.73
1	0.55	0.0	70.69	65.35
1	0.1	0.3	74.92	63.91
3	0.1	0.3	73.69	62.42
2	0.1	0.0	32.19	30.16

coefficient (*K*) and scattering coefficient (*S*), also called color strength (*K/S*) value. One millilitre (1 mL) of 12% coffee and 1 mL of 1% methylene blue are used for staining the fabrics. Stained fabric samples are irradiated for 4 days in sunlight. Self-cleaning action is quantified by comparing *K/S* values of the exposed and unexposed portions of the same stain. Per cent decrease in *K/S* value of exposed part is calculated using the following relationship:

$$\frac{K/S_{unexposed} - K/S_{exposed}}{K/S_{unexposed}} \quad \dots (1)$$

## 2.4 Antibacterial Assessment of Photocatalyst- treated Fabric

Quantitative antibacterial testing of treated samples is performed by dynamic shake flask method on bacteria *Bacillus subtilis*. A 2.5cm×2.5cm sample is dipped in nutrient broth with bacterial concentration of 5.6×10<sup>7</sup> CFU/ml. Flask is shaken for 24h at the rate of 200 rpm at 37°C. Serial dilution of bacterial culture is made, and 100µL solution from each dilution is spread on agar plate. Dilution of 10<sup>-6</sup> on an agar plate incubated for next 24h is used to count bacterial colonies for full bacterial growth<sup>15</sup>. Reduction in bacterial growth is calculated using the following equation:

$$\text{Reduction in bacterial growth (\%)} = \frac{A-B}{A} \times 100 \quad \dots(2)$$

where *A* is the bacterial colony count in untreated fabric; and *B*, the bacterial colony counts in treated fabric.

### 3 Results and Discussion

#### 3.1 Morphological and Structural Analysis of Photocatalysts

Morphology of prepared nanomaterials is assessed by Field Emission Scanning Electron microscopy. FESEM of synthesized 1% Ag-N TiO<sub>2</sub> (Fig. 1) illustrates the size of prepared nanomaterial and its aggregates. As observed from the image, particle size of prepared nanoparticles is much below 100nm.

XRD analysis carried out on Panalytical X-ray diffractometer confirms TiO<sub>2</sub> with clear characteristic peaks at 101, 004, 200, 105 and 204 corresponding to  $2\theta = (25.24^\circ, 37.79^\circ, 47.99^\circ, 54.12^\circ \text{ and } 62.89^\circ)$  as shown in Fig. 2. All peaks are in agreement with standard TiO<sub>2</sub> peaks for anatase structure (JCPDS no.: 88-1175 and 84-1286). Further, the peak intensity tends to decrease with the increase in doping amount and the peak at  $37.8^\circ$  indicates the presence of silver. Low intensity peaks show a little shift in the spectrum which may be due to the presence of Ag doping. Reduced graphene oxide (rGO) shows a characteristic peak at  $27.82^\circ$ . Nanocomposite of rGO/Ag-N TiO<sub>2</sub> shows respective characteristic peaks of rGO and Ag-N TiO<sub>2</sub> whereas the intensity of characteristic peaks tends to decrease in nanocomposite which shows that each component affects the other chemically. Crystallite size is calculated with the help of following Debye-Scherrer formula:

$$D_c = \frac{0.89\lambda}{\beta \cos\theta} \quad \dots(3)$$

where  $D_c$  is the crystallite size;  $\lambda$ , the X-ray wavelength corresponding to Cu K $\alpha$  radiation;  $\beta$ , the stands for the FWHM of anatase peak (101) obtained by XRD; and  $\theta$ , the diffraction angle with characteristic peak (101). The average size of nanocrystals of 1%Ag-N TiO<sub>2</sub>, 2%Ag-N TiO<sub>2</sub>, and 3%Ag-N TiO<sub>2</sub> is found to be around 23.21nm, 17.67nm and 17.32nm respectively, as calculated by Debye-Scherrer formula.

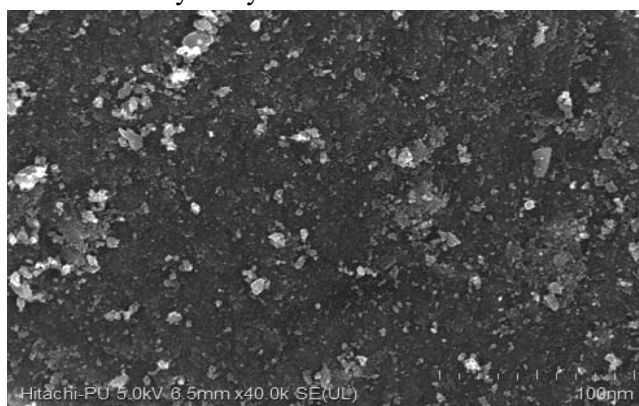


Fig. 1 — FE-SEM image of synthesized 1%Ag-N TiO<sub>2</sub>

UV-visible spectroscopy is carried out on Analytik Jena UV– spectrophotometer. Samples are prepared by putting a layer of nanoparticles over the standard powder i.e. Barium Sulfate (BaSO<sub>4</sub>). It is observed that with increase in doping, absorbance decreases in the visible region (Fig. 3). UV spectroscopy results are depicted in Figure 3 that clearly shows enhancement of light absorbance by nanocomposite than its

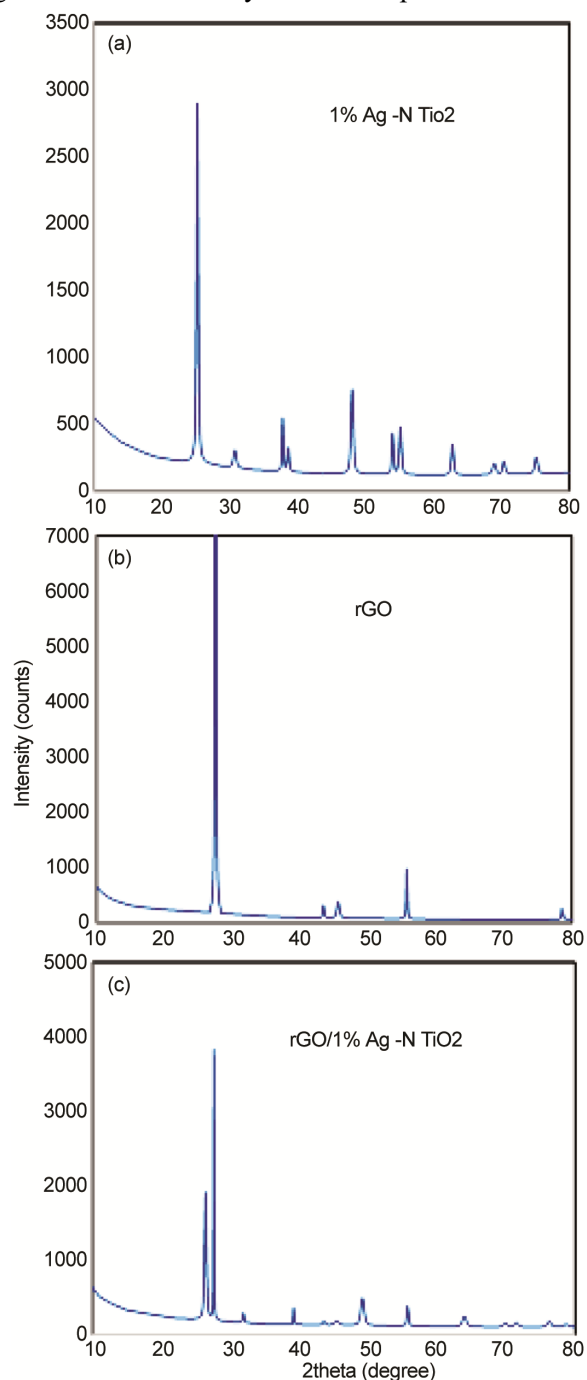


Fig. 2 — XRD images of (a) 1% Ag-N doped TiO<sub>2</sub>, (b) rGO, and (c) nanocomposite of rGO/1%Ag-N TiO<sub>2</sub>

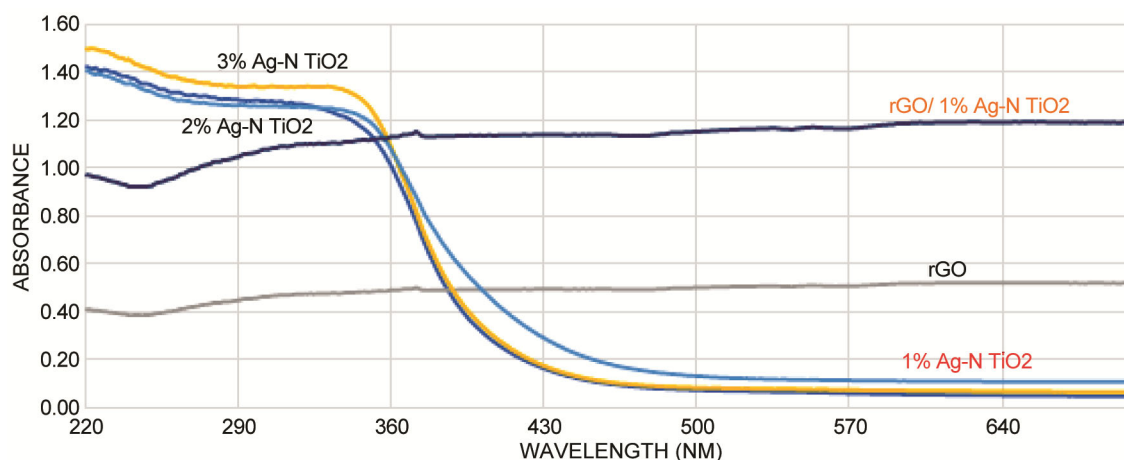


Fig. 3 — UV-Visible spectroscopy of 1%Ag-N TiO<sub>2</sub>, 2%Ag-N TiO<sub>2</sub>, 3%Ag-N TiO<sub>2</sub>, rGO, and rGO/1%Ag-N TiO<sub>2</sub>

counterparts. Silver helps in charge separation, thereby restrains the electron hole pair recombination by bonding with the unpaired electron of the conduction band of TiO<sub>2</sub>. Therefore, increased absorption in the region 350-500 nm is observed that may be due to plasmonic resonance, whereas nitrogen is responsible for decreasing the band gap by overlapping of nitrogen 2p orbital with oxygen 2p orbital of TiO<sub>2</sub>. Increased doping creates hindrance for light to reach out to TiO<sub>2</sub> crystals and therefore the absorption decreases, which is well agreed with the other studies<sup>16-18</sup>. rGO shows higher absorbance in visible regions due to its inherent photocatalytic properties for its conjugated and nanosheet like structure. However, rGO/Ag-N TiO<sub>2</sub> nanocomposite shows excellent absorption in visible regions as well, which is much higher than the doped TiO<sub>2</sub> absorbance value. It may be due to the strong electronic interaction between the two components and lesser band gap of rGO.

Moreover, nanocomposite shows lower band gap as compared to its parent particles. rGO has a band gap of 2.95 eV and 1%Ag-N TiO<sub>2</sub> have 2.86 eV, whereas nanocomposite shows a band gap of 2.3 eV. Addition of graphene in TiO<sub>2</sub> causes red shift in its absorption spectrum as graphene acts as electron scavenger, being a conjugated structure, whereas silver and nitrogen doping causes effective decrease in band gap in TiO<sub>2</sub> (Table 2), leading to enhancement of photo response to a longer wavelength. However, TiO<sub>2</sub> in conjugation with rGO shows a high amount of decrease in band gap, leading to higher amount of visible light absorption and effective separation of electron-hole pairs, causing enhanced photocatalytic activity.

FTIR is carried out on Aligent Technologies Cary 630 Spectrophotometer, as depicted in Fig. 4. In 1%

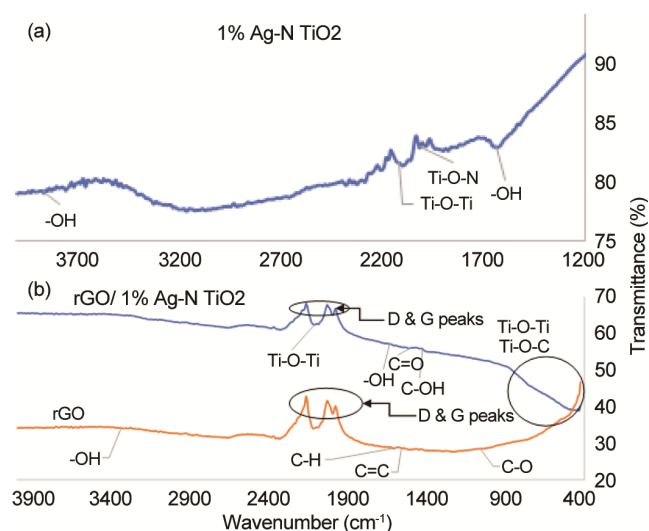


Fig. 4 — FTIR findings of (a) 1% Ag-N TiO<sub>2</sub> and (b) rGO & rGO/1% Ag-N TiO<sub>2</sub>

Table 2 — Band gaps of 1%Ag-N TiO<sub>2</sub>, 2%Ag-N TiO<sub>2</sub>, 3% Ag-N TiO<sub>2</sub>, rGO and rGO/1%Ag-N TiO<sub>2</sub>

Particles	Band gap, eV
1%Ag-N TiO <sub>2</sub>	2.86
2%Ag-N TiO <sub>2</sub>	2.94
3%Ag-N TiO <sub>2</sub>	2.97
rGO	2.95
rGO/1%Ag-N TiO <sub>2</sub>	2.3

Ag-N TiO<sub>2</sub>, O-H bonding and O-H vibrations are respectively observed in the regions 1635 cm<sup>-1</sup> and 3861 cm<sup>-1</sup> due to adsorbed water molecules and hydroxyl ions. Ti-O-Ti and Ti-O-N peaks have been observed at 2113 cm<sup>-1</sup> and 2017 cm<sup>-1</sup> respectively. rGO nanoparticles have shown characteristic peaks at 3334 cm<sup>-1</sup>, 1635cm<sup>-1</sup>, 1554 cm<sup>-1</sup>, and 1030 cm<sup>-1</sup> for groups -OH, C-H, C=C and C-O respectively.

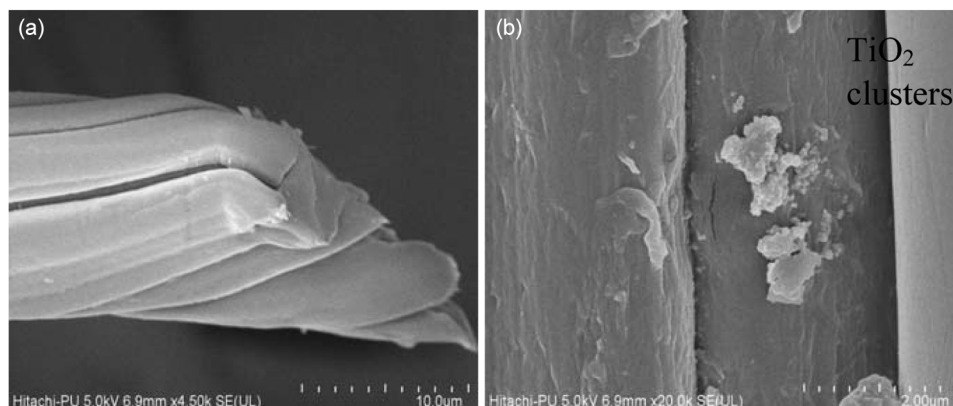


Fig. 5 — FE-SEM of (a) untreated fabric and (b) coated fabric

rGO/1% Ag-N doped  $\text{TiO}_2$  shows characteristic band in the region below  $1000\text{ cm}^{-1}$  and the presence of a new absorption peak below  $1000\text{ cm}^{-1}$  is observed for the rGO/1%Ag-N  $\text{TiO}_2$  nanocomposite, corresponding to the vibration of the Ti–O–Ti bond and Ti–O–C bond<sup>19-21</sup>. rGO/1%Ag-N  $\text{TiO}_2$  nanocomposite has shown peaks at  $2113\text{ cm}^{-1}$ ,  $1635\text{ cm}^{-1}$ ,  $1546\text{ cm}^{-1}$ ,  $1501\text{ cm}^{-1}$  and  $1441\text{ cm}^{-1}$  attributing Ti-O-Ti, -OH, C=C, C=O and C-OH peaks respectively<sup>22-24</sup>. All the peaks match well with already published literature.

### 3.2 Assessment of Photocatalysts Treated Fabrics

Field emission scanning electron microscopy image shows the surface morphology of nanocomposite onto the fabric surface. Figure 5(a) shows untreated fabric surface and Fig 5(b) shows surface of rGO/1%Ag-N  $\text{TiO}_2$  coated fabric. It is clear from the images that nanocomposite is coated onto the fabric surface. rGO can be seen in the form of nanosheets stacked to the fibres and Ag-N  $\text{TiO}_2$  nanoparticles are seen above the rGO surface. It may be due to the morphology of graphene nanosheets, that deposits onto the fabric in the form of layered structure.

### 3.3 Effect of Photocatalysts on Self-cleaning Activity of Finished Fabrics

Results are analysed using design expert 7.0 and backward elimination method. Trend of the self-cleaning activity is assessed for coffee stain [Fig. 6(a)] and methylene blue stain [Fig. 6(b)]. Amount of doping has insignificant effect if compared with the effect of rGO and Ag-N  $\text{TiO}_2$ . At the lowest value (0%) of rGO, % decrease in  $K/S$  value due to the amount of Ag-N  $\text{TiO}_2$  has a linear increase at a constant rate up to its highest value. On the other hand, at the highest value of rGO (1%), % decrease in  $K/S$  value due to the amount of Ag-N  $\text{TiO}_2$  is at lower rate. % decrease in  $K/S$  value

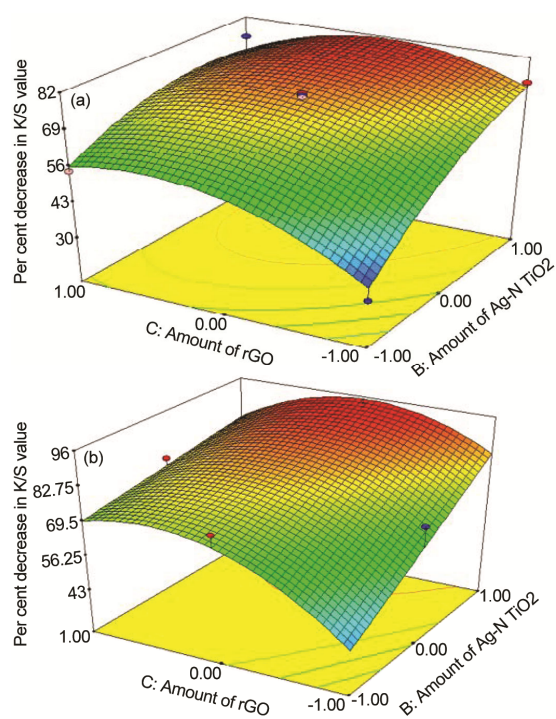


Fig. 6 — Surface plot for % reduction in  $K/S$  value of (a) coffee stain, and (b) methylene blue stain after irradiation

increases and then decreases as the amount of rGO increases. However, the rate of decrease is faster at lower value of Ag-N  $\text{TiO}_2$ .

Photocatalytic activity is highest with 0.3% rGO and it further decreases with increase in rGO amount. Higher amounts of rGO nanosheets are restricting the path of light to reach out to Ag-N  $\text{TiO}_2$  nanoparticles causing effective decrease in photocatalytic activity. Amount of Ag-N  $\text{TiO}_2$  has the highest contribution in % reduction in  $K/S$  value for coffee (43.62%) as well as for Methylene blue stain (63.03%) as shown in Table 3. rGO has a contribution of 11.72% and 8.55%, whereas rGO<sup>2</sup> has contribution of 25.3% and

Table 3 — ANOVA for per cent reduction in *K/S* value of coffee and methylene blue stain

Source	DF	Seq SS	% Contribution	Adj SS	Adj MS	F-value	P-value
<b>Coffee</b>							
Linear	2	1543.64	55.34	1543.64	771.82	22.55	0
Amount of Ag-N TiO <sub>2</sub> (B)	1	1216.72	43.62	1216.72	1216.72	35.55	0
Amount of rGO (C)	1	326.91	11.72	326.91	326.91	9.55	0.011
Square	1	707.15	25.35	707.15	707.15	20.66	0.001
Amount of rGo* Amount of rGo	1	707.15	25.35	707.15	707.15	20.66	0.001
2-way interaction	1	196.28	7.04	196.28	196.28	5.73	0.038
Amount of Ag-N TiO <sub>2</sub> * Amount of rGO	1	196.28	7.04	196.28	196.28	5.73	0.038
Error	10	342.27	12.27	342.27	34.23		
Lack-of-fit	8	340.54	12.21	340.54	42.57	49.3	0.02
Pure error	2	1.73	0.06	1.73	0.86		
Total	14	2789.34	100				
<b>Methylene blue</b>							
Linear	2	1447.07	63.03	1447.07	723.53	41.33	0
Amount of Ag-N TiO <sub>2</sub> (B)	1	1250.75	54.48	1250.75	1250.75	71.44	0
Amount of rGO (C)	1	196.32	8.55	196.32	196.32	11.21	0.009
Square	2	556.88	24.26	556.88	278.44	15.9	0.001
Amount of Ag-N TiO <sub>2</sub> * Amount of Ag-N TiO <sub>2</sub>	1	108.81	4.74	142.01	142.01	8.11	0.019
Amount of rGO* Amount of rGO	1	448.06	19.52	448.06	448.06	25.59	0.001
2-way interaction	1	134.21	5.85	134.21	134.21	7.67	0.022
Amount of Ag-N TiO <sub>2</sub> * Amount of rGO	1	134.21	5.85	134.21	134.21	7.67	0.022
Error	9	157.57	6.86	157.57	17.51		
Lack-of-fit	7	159.71	6.83	159.71	22.39	52.06	0.019
Pure error	2	0.86	0.04	0.86	0.43		
Total	14	2295.73	100				

19.2% respectively in % decrease of *K/S* value for coffee and methylene blue stain. Interaction of amount of Ag-N TiO<sub>2</sub> and amount of rGO have contribution of 7.04% and 5.85% for % decrease in *K/S* value of coffee and methylene blue stain respectively. However, the amount of Ag-N TiO<sub>2</sub> has a contribution of 4.74% in per cent decrease of *K/S* value of methylene blue stain.

Regression equation for % decrease in *K/S* value of coffee stain is given below:

$$\begin{aligned} \text{Per cent decrease in } K/S \text{ value of coffee stain} = & 81.2221 + -0.973358 * A + 12.4 * B + 6.69413 \\ & * C + -0.332836 * AB + -0.105 * AC + -7.38259 \\ & * BC + 4.52083 * A^2 + -2.8729 * B^2 + - \\ & 13.6642 * C^2 \quad \dots(4) \end{aligned}$$

Regression equation for % decrease in *K/S* value of methylene blue stain is given below:

$$\begin{aligned} \% \text{ decrease in } K/S \text{ value of methylene blue stain} = & 73.5433 + -0.900721 * A + 12.5037 * B + \\ & 5.24951 * C + 0.164428 * AB + -0.125 * AC + - \\ & 5.9153 * BC + 3.62292 * A^2 + -4.70122 * B^2 \\ & + -10.7046 * C^2 \quad \dots(5) \end{aligned}$$

#### 3.4 Effect of Photocatalysts on Antibacterial Activity of Finished Fabrics

Assessment of antibacterial activity is done as per Eq. (2). Bacterial colonies are counted in untreated as well as in treated fabrics. Figure 7(a) shows the antibacterial activity in rGO/0.55% Ag-N TiO<sub>2</sub> treated, whereas Fig. 7(b) shows untreated fabric.

Increase in antibacterial performance of nanocomposite may be attributed to the fact that TiO<sub>2</sub> contains hole as a positive charge site, while bacteria is negatively charged which leads to the oxidation of bacteria and results in its death, whereas silver ions may take part in catalytic oxidation reactions between oxygen molecules in the cell and hydrogen atoms of thiol groups(R-SH), thus leading to blocking of respiration of bacteria and its death. Maximum

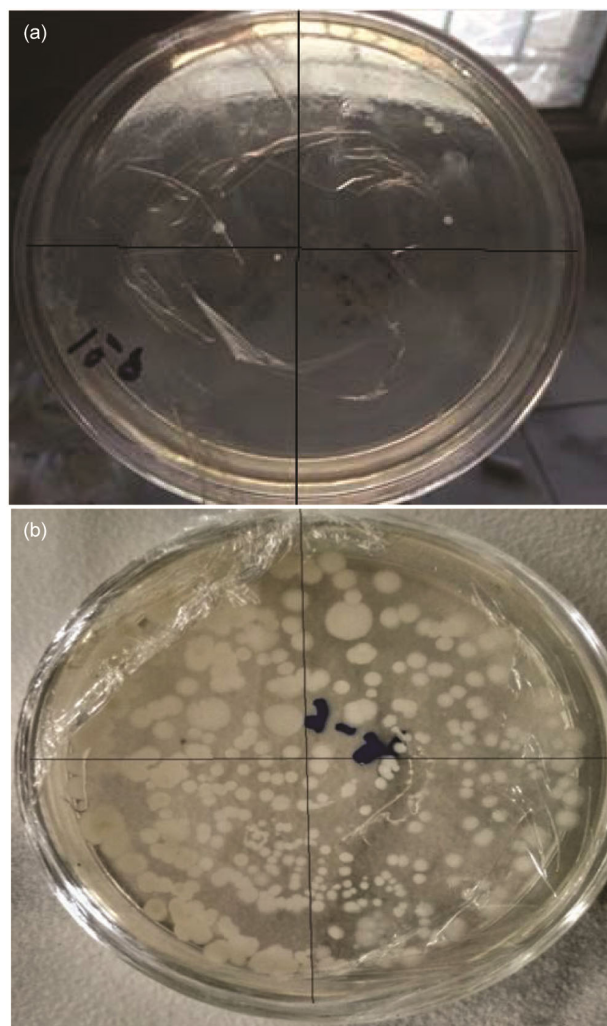


Fig. 7 — Antibacterial Activity of (a) 0.55% Ag-N TiO<sub>2</sub> (b) untreated sample

antibacterial activity of 97.32% is obtained in 0.55% Ag-N TiO<sub>2</sub>/0.6% rGO (owf). Nanocomposite, whereas minimum antibacterial activity of 75.46 % is obtained when only 0.55% Ag-N TiO<sub>2</sub> is used, suggesting that rGO contribution is more in case of anti-bacterial activity of nanocomposite. Another mechanism of the antimicrobial activity of silver nanoparticles is related to the formation of free radicals and consequent free-radical-induced oxidative damage of the cell membranes of bacteria. However, rGO acts as an oxidizing agent and an electron scavenger, which leads to killing of bacteria. In combination, all three effects are resulting in effective reduction in bacterial growth.

#### 4 Conclusion

Samples are prepared by a simple method of mixing and sonication for coating on polyester/cotton fabric

with rGO/Ag-N doped titanium dioxide nanocomposite to produce multifunctional textiles. Coating of rGO/Ag-N doped titanium dioxide nanocomposite on the polyester/cotton fabrics created functional characteristics including photocatalytic self-cleaning and antimicrobial properties. All properties of coated fabrics with rGO/Ag-N doped titanium dioxide nanocomposite is found superior as compared to untreated samples. Through XRD patterns, UV-Visible spectroscopy, FE-SEM and FT-IR spectra, the characterization of rGO/Ag-N doped titanium dioxide nanocomposite is confirmed. Treated fabrics show enhanced self-cleaning and antibacterial activity. It is expected that the rGO/Ag-N TiO<sub>2</sub> nanocomposite can be used to produce high performance fabrics. It is also observed that the amount of doping has least impact as compared to the impact of Ag-N TiO<sub>2</sub> and amount of rGO on photocatalytic as well as antibacterial performance of treated fabrics.

#### References

- Behzadnia A, Montazer M, Rashidi A & Mahmoudi R M, *Photochem Photobiol*, 90 (2014) 1224.
- Heller A, *Accounts Chemi Res*, 28 (1995)503.
- Sunada K, Kikuchi Y, Hashimoto K & Fujishima A, *Environ Sci Technol*, 32 (1998) 726.
- Ollis D & Al-Ekabi H, *Proceedings, 1<sup>st</sup> International Conference on TiO<sub>2</sub> Photocatalytic Purification and Treatment of Water and Air* (Elsevier Sci Limit), 1993.
- Geim A K & Novoselov K S, *Nature Materials*, 6 (2007) 183.
- Dreyer D R, Park S, Bielawski CW & Ruoff R S, *Chem Soc Rev*, 39 (2010) 228.
- Zhu Y, Murali S, Cai W, Li X, Suk J W, Potts J R & Ruoff R S, *Adv Materials*, 22 (2010) 3906.
- Karimi L, Yazdanshenas E, Khajavi R, Rashidi A & Mirjalili M, *J Text Inst*, 107 (2015) 1122.
- Ali S W, Purwar R, Joshi M & Rajendran S, *Cellulose*, 21 (2014) 2063.
- Stan M S, Badea M A, Pircalabioru G G, Chifiriuc M C, Diamandescu L, Dumitrescu, I, Trica B, Lambert C & Dinischiotu A, *Materials Sci Eng [C]*, 94 (2019) 318.
- Simonsen M E & Søgaard E G, *J Sol-Gel Sci Technol*, 53 (2009) 485.
- Kang O L, Ahmad A, Rana U A & Hassan N H, *Nanotechnol*, (2016) 1.
- Lim CS, Ryu J H, Kim D H, Cho SY & Oh WC, *J Ceramic Processing Res*, 11 (2010) 736.
- Harikishore M, Sandhyarani M, Venkateswarlu K, Nellaippan T A & Rameshbabu N. *Procedia Mat Sci* , 6 (2014) 557.
- Marques J, Gomes T D, Forte M A, Silva R F & Tavares C J, *Cataly Today* 326 (2019) 36.
- Viswanathan B & Krishanmurthy K R, *Photoenergy*, (2012) 1.
- Kment S, Kmentova H, Hubicka Z, Olejnicek J, Cada M & Krysa J, *Res Chem Int*, 41 (2015) 9343.
- Khan M, Gul S R, Li J & Cao W & Mamalis A G, *Mater Res Exp*, 2 (2015), 66201.

- 19 Yu J, Yu H-G, Cheng B, Zhao X-J, Yu J C & Ho W-K, *J Phys Chem B*, 107 (2003) 13871
- 20 Wang P, Wang J, Wang X, Yu H, Yu J, Lei M & Wang Y, *Appl Catal B Environ*, 132 (2013) 452.
- 21 Min Y, Zhang K, Chen L, Chen Y & Zhang Y, *Synth Met*, 162 (2012) 827.
- 22 Lopez Goerne, T, *Nanomed & Nanotech*, 5 (2011) 1.
- 23 Stan M S, Nica I C, Popa M, Chifiriuc M C, Iordache O, Dumitrescu I, Diamandescu L & Dinischiotu A, *Indus Text*, 49 (2018) 277.
- 24 Rani N, Ananda S & Rangappa D, *Mater Today: Proceedings*, 4 (2017) 12300.